Isomerism and Solvent Interaction in Octamethyl Calix[4]pyrrole Complexed with Formate

Lane M. Terry,[a] *Madison M. Foreman,*[a] *and J. Mathias Weber*[a,*]

[a] JILA and Department of Chemistry, University of Colorado, 440 UCB, Boulder, CO 80309-0440, USA.

ABSTRACT.

We investigate the binding motifs of host-guest complexes of the anion receptor octamethyl calix[4]pyrrole (omC4P) with the formate anion using cryogenic ion vibrational spectroscopy in concert with density functional theory. The resulting IR spectrum in vacuo is compared to that in deuterated acetonitrile and acetone solutions. The combination of the strong host-guest interaction and the charge distribution that the formate ion presents to the chemical environment results in a complex behavior of the NH stretching features in the two solvents. The formate-omC4P complex has three low energy isomers in vacuo:(i) one with an oxygen atom of formate interacting with three of the NH groups of omC4P and the other oxygen atom interacting with the remaining NH group; (ii) one with a single oxygen atom of formate interacting with all four NH groups of omC4P; and (iii) one with each oxygen atom interacting with two NH groups. Each complex geometry lowers the C_{4v} symmetry of the receptor to C_1, C_s, or C_{2v}, respectively, and this symmetry breaking and isomerism is reflected in the broadening and pattern of the NH stretching modes of omC4P.

TOC Graphic

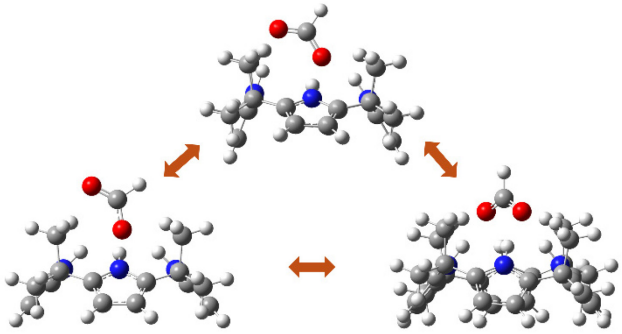

Introduction

The molecular recognition of anions is important to many applications of chemistry,[1-3] for example, in advancing materials science,[4] the sensing of anionic pollutants from agricultural or industrial runoff,[5-7] or the regulation of anion transport across cell membranes.[8-10] To design an effective synthetic molecular anion receptor, and to optimize the selectivity of the receptor to a given anion, a complete understanding of the noncovalent interactions in the receptor-ion host-guest complex and the competing effects of solvation is needed. A receptor typically has a binding site whose size, shape, and chemical composition—along with the size and shape of the anion—determine the ion-receptor interaction, the binding geometry and concomitant solvent exposure of the bound ion. These factors are instrumental in understanding the selectivity and binding efficiency of a given anion receptor.

Calix[4]pyrroles constitute a class of anion receptors that has gained popularity over the past two decades,[11-15] after they were first synthesized in 1886 by Baeyer.[16] The simplest version of these receptors is octamethyl calix[4]pyrrole (omC4P), a macrocyclic molecule consisting of four pyrrole groups connected by fully substituted sp^3 *meso*-carbons (see Figure 1). The four NH groups of the pyrrole rings form a binding site in the presence of an anion, yielding a receptor with C_{4v} symmetry in the case of a spherical anion.[15] In addition to the four hydrogen bonds (H-bonds) interacting with an anion, the receptor also forms a concave binding site for cations, allowing for ion pair bonding, especially in less polar solvents.[17]

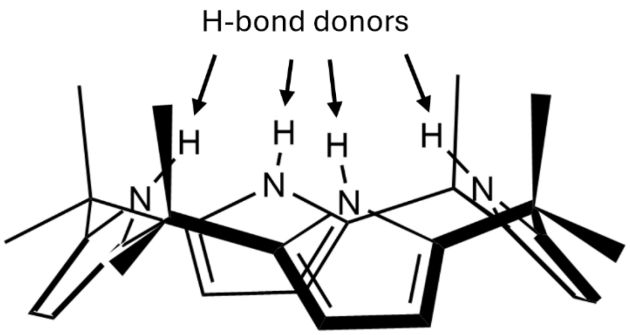

Figure 1. Generic structure of the omC4P binding site with arrows indicating the H-bond donors. We note that this is not the lowest energy configuration of bare omC4P, but the conical conformation omC4P adopts in the presence of a H-bond acceptor, e.g. an anion or solvent.

The four H-bonds between the ion and receptor dominate the interaction between the guest anion and the omC4P host. The NH stretching frequencies of the host are directly affected by the presence of the bound ion and thus serve as sensitive probes of the ion-receptor interaction, suggesting that infrared (IR) spectroscopy will be a useful approach for the characterization of host-guest interactions. While IR spectra in suitable solvents yield important information on the structures and intermolecular forces of such host-guest complexes, they cannot provide a separate probe of ion-receptor interactions and effects of ion solvation by themselves. In order to disentangle those different but critical aspects, a comparison of vibrational spectra in solution with those in vacuo is needed. A successful technique in the characterization of gas-phase mass-selected ions is cryogenic ion vibrational spectroscopy (CIVS) in combination with quantum chemical calculations.[15, 18-21] This technique has been used to investigate ion-receptor interactions in complexes of omC4P with halide ions[15] and with the nitrate anion.[22] In this work, we present vibrational spectra of omC4P complexed with the formate anion in vacuo and in solution and

interpret the experimental spectra using density functional theory (DFT) to explore the effects of anion shape, size, and proton affinity upon introduction of an ion to omC4P.

Methods

Equimolar amounts of omC4P (ChemScene) and formic acid (Sigma-Aldrich) were added to a 1:1 mixture of acetonitrile (Thermo Fisher Scientific) and water to prepare a 0.1 mM solution of formate-omC4P, $HCOO^{-}\cdot$omC4P. All chemicals were used as purchased without further purification. The experimental apparatus has been described in detail in previous work.[23] Upon electrospray ionization (ESI), droplets containing $HCOO^{-}\cdot$omC4P entered a heated desolvation capillary (80°C). The ions resulting from desolvation passed through a skimmer and a series of octopole ion guides and ion optics which routed them through several differential pumping stages and into a 3D Paul trap. The trap is mounted on a closed cycle He cryostat held at ca. 30 K. Here, the ions were cooled by collisions with buffer gas (10% D_2 in He), and neutral messenger tags using residual N_2 from the source inlet were condensed onto the ions, generating tagged complexes of the form $HCOO^{-}\cdot$omC4P$\cdot N_2$. The ions were extracted from the trap and injected into a Wiley-McLaren time-of-flight mass spectrometer (TOF-MS) every 50 ms. The ions of interest, $HCOO^{-}\cdot$omC4P$\cdot N_2$, were mass selected using a pulsed mass gate, and every other ion package was irradiated with the output of a tunable IR OPO-OPA system (LaserVision) in a multipass cell. Photon absorption and subsequent intramolecular vibrational relaxation resulted in dissociation of the N_2 tag from the formate-omC4P ion and formation of photofragments according to the reaction

$$HCOO^{-}\cdot\text{omC4P}\cdot N_2 + \hbar\omega_{IR} \rightarrow HCOO^{-}\cdot\text{omC4P} + N_2.$$

Remaining tagged ions were separated from the photofragments by a two-stage reflectron, and the fragment ions were detected on a microchannel plate detector. Fragment ion formation was

monitored as a function of the wavelength and corrected for photon fluence and background from unimolecular decay to acquire a relative photofragmentation yield. To ensure reproducibility and improve signal-to-noise ratio, photodissociation spectra from multiple days were averaged, then calibrated using the known spectrum of acetone,[24] which was measured in a home-built photoacoustic spectrometer.

For measurements in the condensed phase, equimolar amounts of omC4P and cesium formate (Thermo Scientific) were dissolved in CD_3CN (Thermo Scientific Chemicals) and $(CD_3)_2CO$ (Cambridge Isotope Laboratories) to prepare 10 mM solutions. Using a Thermo Scientific Nicolet iS5 FTIR spectrometer and an Infrasil cylindrical cell with 0.2 mm path length (Starna Cell), Fourier Transform infrared (FTIR) spectra of each solution were obtained.

Density functional theory (DFT)[25] using the B3LYP functional[26, 27] with cc-pVDZ basis sets[28] for all atoms was used to calculate structures and vibrational spectra of $HCOO^-$·omC4P. A geometry search using multiple orientations of the formate ion inside the omC4P binding pocket was used to determine the lowest energy isomers of the complex. The search began with a configuration in which two oxygen atoms were pointed into the pocket, as seen in nitrate-omC4P.[22] Then, one oxygen atom was pulled out of the pocket, changing the O-O axis in 5-degree steps until a configuration with one oxygen atom centered in the binding site was achieved. In each step, all internal coordinates except the O-O angle relative to the plane of the NH groups were allowed to relax. To generate the calculated IR spectrum for each isomer, the calculated lines were broadened by Lorentzian line shapes with 8 cm^{-1} full width at half maximum, and the harmonic frequencies were scaled by 0.9577 to match the *e* mode NH stretching frequency in the experimental spectrum of chloride-omC4P[15] calculated with the same method. The anharmonic frequency of mode 207 (the lowest frequency NH stretching mode) in the two lowest energy isomers was calculated using

second order vibrational perturbation theory[29] (VPT2) as implemented in Gaussian 16.[30] The binding energy of formate to omC4P was calculated including the counterpoise correction,[31, 32] natural bond orbital (NBO) analysis was done using Gaussian NBO Version 3.1,[33] and solvation effects were modeled using a polarizable continuum model (PCM).[34] All calculations were done using Gaussian 16.[30]

Results and Discussion

The formate anion can bind to omC4P with different motifs, similar to the previously studied nitrate anion.[22] Figure 2 shows the three lowest calculated minimum energy structures. Isomer A has one of the two O atoms in $HCOO^-$ tipped into the binding site and interacting with three of the four NH groups of omC4P; the other oxygen is tipped upward but still interacts with the remaining NH group. This configuration is similar to the X-ray crystal structure of L-proline bound to an aryl-extended C4P receptor[9] and can likely be extrapolated to other carboxylate containing molecules or ions. Isomer B is calculated to be 29 meV higher than the zero-point corrected energy of isomer A and has one of the two O atoms in $HCOO^-$ pointing into the binding site and interacting with all four NH groups of omC4P. Isomer C is calculated to be 7 meV higher in energy than isomer B and has each O atom interacting with two of the four pyrrole NH groups. Each $HCOO^-$·omC4P isomer breaks the C_{4v} symmetry of the omC4P receptor, shifting to C_1 in isomer A, C_s symmetry in isomer B, and C_{2v} symmetry in isomer C. The symmetry lowering is a result of the ion shape and the subsequent distortion of the macrocycle to accommodate for it.

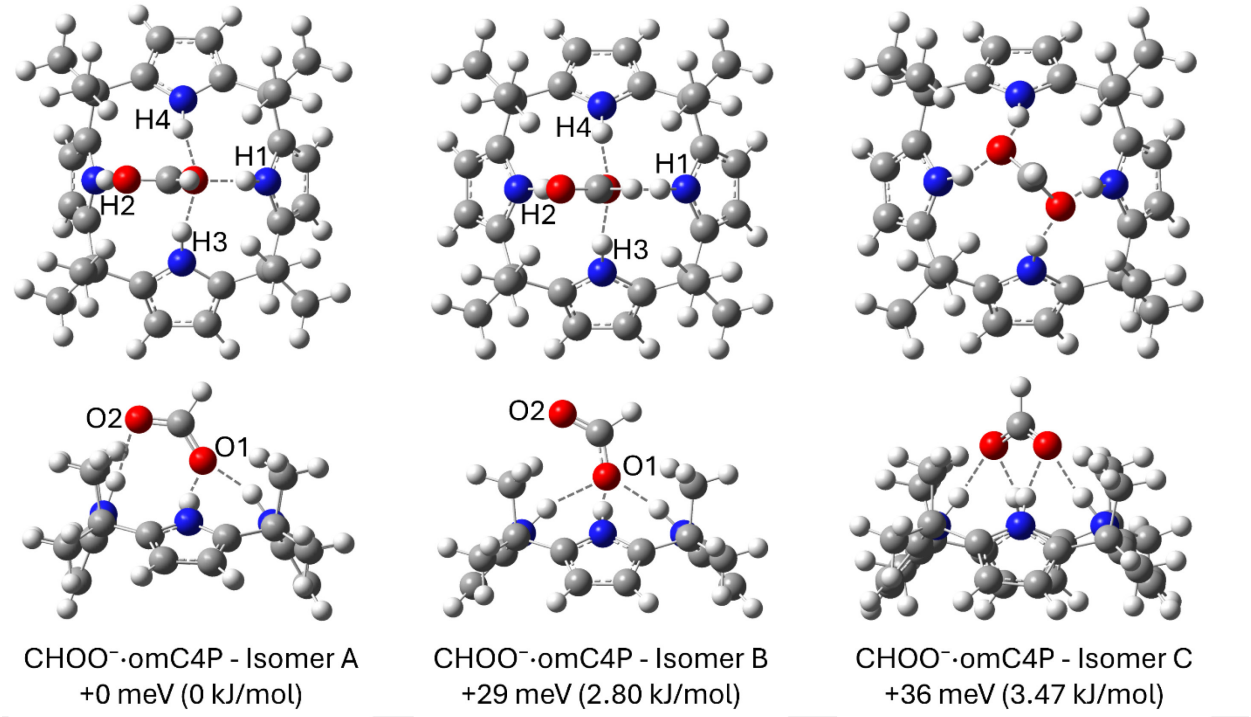

Figure 2. Calculated structures of $HCOO^-$·omC4P complexes in the gas phase. For each isomer, the zero-point corrected relative energies are given. A top view along the symmetry axis of the omC4P receptor and a side view of each complex is shown. C = gray, H = white, N = blue, O = red. Dashed lines represent hydrogen bonds. Select atoms labeled for reference in main text.

Selected properties of each isomer are summarized in Table 1. In isomer A, the formate anion sits asymmetrically in the omC4P binding pocket with one O atom tipped into the pocket, interacting with three NH groups, and one O atom tipped out of the pocket and binding to one NH group. The O atom inside the pocket is pulled closer to the NH group in plane with the $HCOO^-$ and has a H-bond length of 176 pm, sitting almost centered (198.9 and 199.2 pm) between the out-of-plane NH groups. We note that starting in a similar geometry, but enforcing C_s symmetry, did not yield a stable structure, and geometry optimization without symmetry restriction always resulted in a structure with C_1 symmetry. In isomer B, the H-bonded CO group of $HCOO^-$ sits

slightly off-center in the binding pocket of omC4P. It is equidistant (189 pm) to the NH groups perpendicular to the plane of the ion, but has H-bond distances of 182 and 200 pm to the in-plane NH groups. The average of all H-bond distances in isomers A and B is 190 pm, which is equivalent to the H-bond distances in isomer B where the ion sits centered in the pocket. This calculated distance from NH groups to the bound O atom(s) is shorter than that of the previously studied nitrate complex (ca. 200 pm).[22] We attribute the difference in H-bond length to the proton affinity of the bound ion; $HCOO^-$ has a higher proton affinity (ca. 1449 kJ/mol)[24] than NO_3^- (ca. 1358 kJ/mol).[35]

Table 1. Selected Calculated Properties of Formate-omC4P Complexes.

Isomer	NH···ion distance [pm]	C-O distance [pm]	charge distribution [a] in ion [e]
A	176[c] [177][b] (O1H1)	128 [128][b] (CO1)	-0.844 [-0.843][b] (O1)
	266[c] [261][b] (O1H2)	124 [125][b] (CO2)	-0.726 [-0.745][b] (O2)
	199[d] [198][b] (O1H3,4)		0.081 [0.097][b] (H)
	196[e] [199][b] (O2H2)		
B	182[c] [185][b] (O1H1)	130 [130][b] (CO1)	-0.872 [-0.863][b] (O1)
	200[c] [197][b] (O1H2)	123 [123][b] (CO2)	-0.675 [-0.710][b] (O2)
	189[d] [191][b] (O1H3,4)		0.075 [0.091][b] (H)
	283[e] [290][b] (O2H2)		
C	190 [190][b]	126 [126][b]	-0.787 e [-0.795e][b] (O)
			0.085 e [0.102e][b] (H)

[a] NBO charges.

[b] Values in square brackets are from calculations using a polarizable continuum model (PCM) with a dielectric constant of acetonitrile (35.688 as implemented in Gaussian 16).

[c] NH group in $HCOO^-$ plane interacting with O1 atom tipped into pocket.

[d] NH group out of $HCOO^-$ plane interacting with O1 atom tipped into pocket.

[e] NH group in $HCOO^-$ plane interacting with O2 atom tipped out of pocket.

The experimental photodissociation spectrum (see Figure 3) suggests population of multiple isomers of $HCOO^-$·omC4P, reflected in the broadening and complexity of the NH stretching features compared to the spectra of omC4P with halides[15] or nitrate[22] and the presence of two peaks in the $HCOO^-$ CH stretching region. Isomers B and C are ca. 30 meV higher in energy than isomer A, and we tentatively assume population of all three isomers due to kinetic trapping as there are large barriers (see Supporting Information) between the isomers, due to their

significant differences in their H-bonding configurations.[36] The broad peak at 3287 cm^{-1} is the signature of the totally symmetric, in-phase linear combination of all four NH oscillators in all isomers. Most of the antisymmetric NH stretching modes of all isomers are contributing to the broad feature at 3250 cm^{-1}. The transitions providing intensity to this feature from isomers A and B are characterized by the NH groups out of the formate plane oscillating out-of-phase with each other while the other NH groups do not participate in the vibration, and a mode at slightly lower frequency with the NH oscillator in the formate plane and close to the free O atom oscillating out-of-phase to the other three NH groups. The lower energy shoulder of this feature is due to the antisymmetric stretching modes of isomer C (b_2 and b_1 symmetry), one with two adjacent NH groups interacting with the same O atom oscillating in-phase and the opposite adjacent pair oscillating out-of-phase, while the other mode has the adjacent NH groups interacting with the same O atom oscillating out-of-phase with each other. The final antisymmetric stretching mode of isomer C, which does not appear in the spectrum, is a symmetry forbidden a_2 mode, in which opposite NH groups oscillate in-phase with each other but out-of-phase with the other opposite pair.

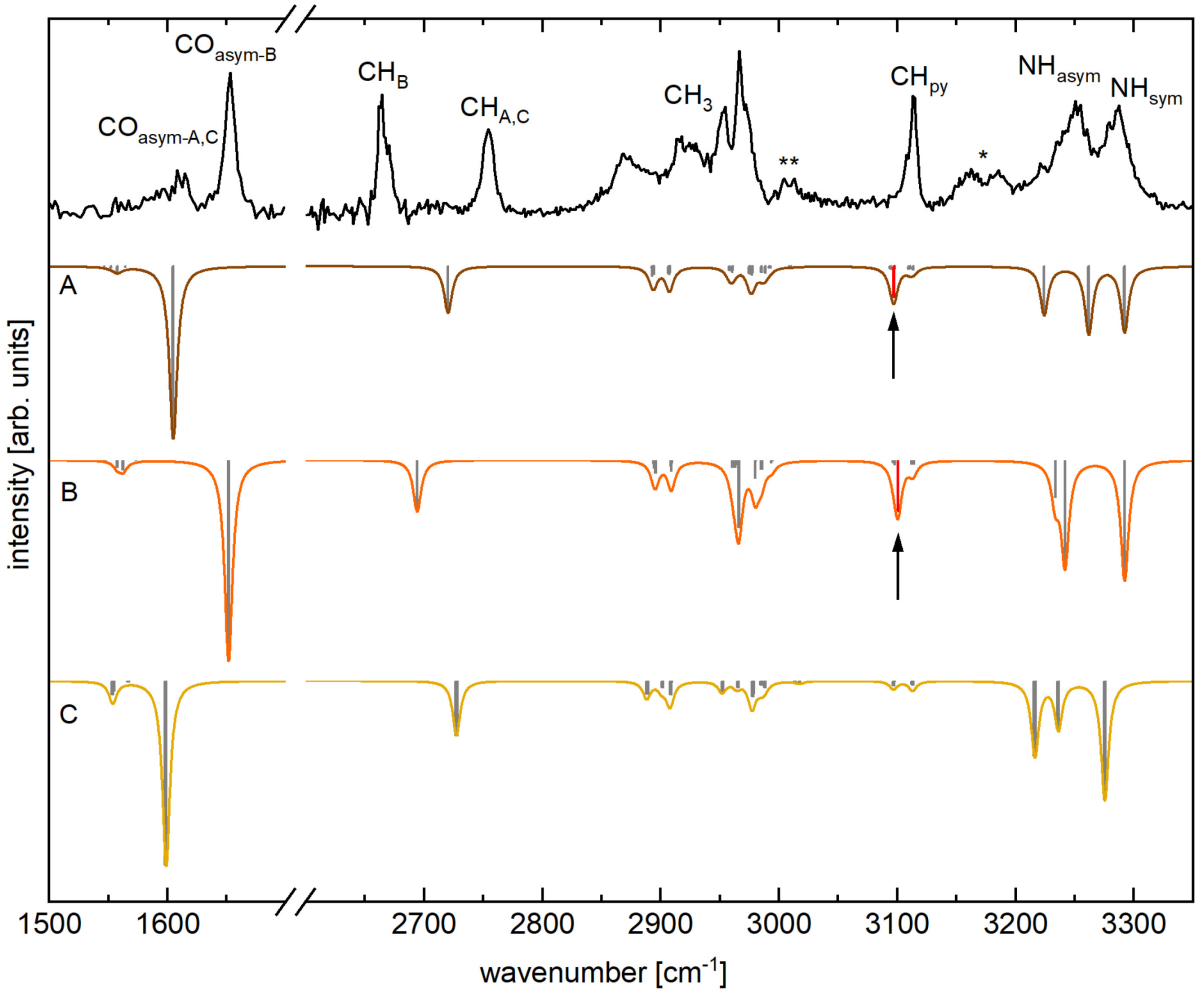

Figure 3. Experimental (upright) and calculated (inverted) IR photodissociation spectra of $HCOO^{-}$·omC4P·N_2. The calculated traces are color coded and labeled for each isomer of the complex. Individual transitions are represented by vertical bars and distinguished based on calculation method (gray: harmonic; red bar). Black arrows indicate a transition treated anharmonically. A single asterisk represents a feature not captured by harmonic calculations. A double asterisk represents features not previously observed in the spectra of omC4P complexes.

The two broad features labeled with an asterisk in Figure 3 around 3175 cm^{-1} are not captured by the harmonic calculations. We assign these features based on previous anharmonic calculations of similar peaks in the spectra of halide-omC4P complexes[15] to overtones and combination bands

of NH wagging modes that gain intensity from Fermi interactions with the neighboring NH stretching modes.

The peak at 3113 cm^{-1} labeled CH_{py} is consistent with the CH stretching modes of the pyrrole groups in the previously published chloride and nitrate complexes.[15, 22] However, in the case of the formate complex, the lowest frequency NH antisymmetric stretching modes of isomers A and B are hidden within this peak. In these isomers, the NH antisymmetric stretching mode in which the NH oscillator in plane with the formate ion and further from or closer to the CH group of formate, respectively, (see Supporting Information for animation) is likely to be strongly anharmonic due a low lying proton transfer channel to the formate ion.[37] Using harmonic approximation calculations, the scaled frequency of this mode is 3177 or 3154 cm^{-1} (see Supporting Information) which is not consistent with the experimental spectrum. When treating the mode anharmonically, it is calculated to be in a similar range as the CH_{py} stretching modes, at 3093 or 3101 cm^{-1}. We therefore assume that both the pyrrole CH stretching modes and the strongly anharmonic NH stretching modes of isomers A and B contribute to the feature at 3113 cm^{-1}.

The cluster of peaks labeled CH_3 from 2850-3000 cm^{-1} forms a congested region, encoding not only the CH stretching modes of the eight methyl groups of the receptor but also containing Fermi resonances of these modes with the overtones and combination bands of the methyl HCH bending modes.[38] The congestion makes a detailed assignment of the region challenging; however, we can assign the group of peaks at 2868 and 2914 cm^{-1} to the linear combinations of the local symmetric CH_3 stretching modes of the methyl groups and the peaks at 2954 and 2966 to linear combinations of the asymmetric stretching modes of the same groups. We note that the latter are affected by the vicinity of the ion, extending to higher frequencies (labeled ** in Figure 3) than in other omC4P complexes,[15, 22] particularly for isomer C. This is due to the much shorter distance of the nearest

methyl H atom to the ion in the present case (220 pm) compared to, e.g., nitrate guest ions (273 pm).[22]

From the point of view of the guest ion, the different isomers are clearly distinguishable in the IR spectrum. Earlier work by Johnson, McCoy, Jordan, and coworkers showed that the CH stretching mode of the formate ion (found at 2449 cm^{-1} for Ar-tagged formate) is quite sensitive to its chemical environment,[39] and our results reflect this sensitivity. The peaks at 2665 cm^{-1} and at 2754 cm^{-1} can be assigned to isomer B and isomers A and C, respectively, although the calculations underestimate the frequency difference of these features.

The OCO stretching modes of the formate ion also show significant differences for the three isomers. The lowest frequency features shown in Figure 3 and Table 2 are associated with antisymmetric OCO stretching vibrations in the formate guest ion, which differ significantly based on binding motif. The calculations recover the frequencies of the two observed peaks in the spectrum quite well, allowing us to assign the peak at 1653 cm^{-1} to the signature of the formate OCO antisymmetric stretching mode in isomer B, while we assign the broad feature centered at 1608 cm^{-1} to the same mode of isomer A and C. We note that the symmetric stretching modes of this group are calculated to be well below the range reported here, around 1289 cm^{-1}, 1230 cm^{-1} and 1325 cm^{-1} for isomers A, B and C, respectively.

Table 2. Selected Experimental, Scaled Harmonic, and Anharmonic Vibrational Frequencies of Formate-omC4P in cm^{-1}.

Experimental	Calculation - Harmonic (Anharmonic)			Characterization
	Isomer A	Isomer B	Isomer C	
1608[a]	1605		1599	OCO antisymmetric – A, C
1653		1652		OCO antisymmetric – B
2665		2694		CH stretch formate – B
2754	2720		2727	CH stretch formate – A, C
2868, 2914[a]	2893, 2908[b]	2894, 2910[b]	2889, 2909[b]	CH_3 symmetric
2954, 2966, 3006[a]	2956, 3011[b]	2960, 2980[b]	2952, 3020[b]	CH_3 asymmetric
3113	3094, 3114	3096, 3112	3097, 3113	CH_{Py} antisymmetric
	3177 (3097)	3154 (3101)		NH antisymmetric – A, B
3250[a]	3224, 3262	3234, 3242	3216, 3236	NH antisymmetric
3287	3292	3292	3275	NH symmetric

[a] Peak centroid.

[b] Range of calculated features with this character.

Figure 4 shows a comparison of the spectra of $HCOO^-$·omC4P in vacuo, in deuterated acetone, and deuterated acetonitrile. One important observation is that the evidence for multiple isomers persists in solution, indicated by the persistence of the CH stretching signatures characteristic of these isomers in the solution spectra. Moreover, apart from the broadening expected for room temperature solutions compared to the CIVS spectrum, there are clear solvent-induced shifts in the solution spectra, observed for nearly all observed features, with significantly different behavior

compared to the cases of nitrate and heavy halide (Cl^- and Br^-) guest ions, where only the NH stretching modes were significantly affected by solvation.[15, 22]

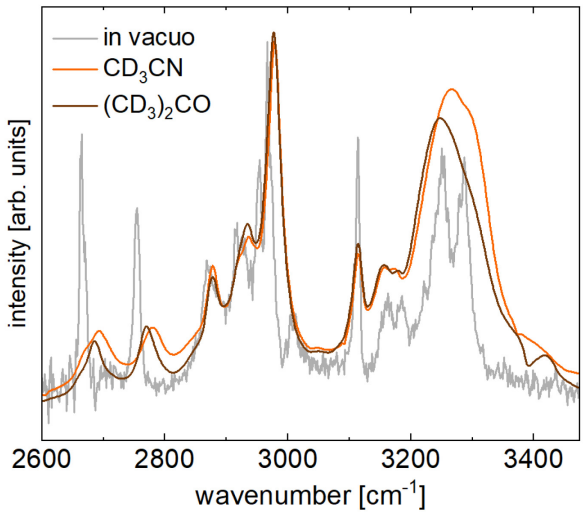

Figure 4. Experimental IR photodissociation spectrum of $HCOO^-$·omC4P (gray) compared to FTIR spectra of 10 mM solutions of the same complex in CD_3CN (orange) and $(CD_3)_2CO$ (brown).

The signature of the higher frequency antisymmetric NH stretching modes in $HCOO^-$·omC4P (and the overall bulk of the NH stretching feature) shows a small red shift in $(CD_3)_2CO$, while the symmetric NH stretching signature exhibits a small blue shift (see Table 3). In contrast, both features are slightly blue-shifted in CD_3CN, with the magnitude of the shifts similar to that in Cl^-·omC4P[15] (10-20 cm^{-1}). Finally, the feature containing the pyrrole CH stretching signatures and the lowest frequency NH stretching mode of isomer A at 3114 cm^{-1} remains unshifted in solution. This is quite different from the solvatochromic behavior of the NH stretching modes in omC4P complexes with Cl^-, Br^-, or NO_3^-, where all solvent induced shifts were towards higher

frequencies,[15, 22] and could be qualitatively explained by a simple electrostatic model as well as DFT calculations including a polarizable continuum model (PCM).[34]

There are two main differences between formate and the other ions mentioned above, (i) the binding energy of the ion-receptor complex, and (ii) the charge distribution that the ion presents to the solvent. The calculated binding energy of the ion-receptor complex for formate is 2.43 eV, 2.60 eV and 2.51 eV for isomer A, B and C, respectively, which is higher than those of nitrate (2.08 eV),[22] bromide (2.04 eV),[15] or chloride (2.37 eV),[15] calculated at similar levels of theory. As a result, one may expect that the influence of the solvent on the geometry of the complex and therefore on the NH stretching frequencies should be smaller than for these ions, which is qualitatively in line with the observations as well as with the calculated geometry changes using PCM calculations (see Table 1). The binding energy of formate is not quite as high as that of fluoride (3.89 eV),[15] where no solvent induced shifts were observed at all. The charge distribution that the formate ion presents to the solvent depends on the isomer (Table 1). In isomers A and B, the O atom closest to the solvent has a slightly higher calculated partial charge than the equivalent O atoms in nitrate,[22] but the latter presents two charged O atoms to the solvent, while the partial charges on the halides are higher, due to their monoatomic nature. In isomer C, the negatively charged O atoms are deeply buried in the binding pocket of the omC4P host, while the H-atom of the formate CH group is facing the solvent with a small positive charge. The resulting forces exerted by the solvent on the bound formate ion can be expected to be smaller than for the other ions based on these qualitative arguments. Together with the higher binding energy of the ion, this can explain the weak solvatochromic effects. The frequency changes from PCM calculations (Table 3) qualitatively capture the observed blue shifts in CD_3CN. The weak red shift of the bulk of the NH stretching signature in $(CD_3)_2CO$ is not explained by simple electrostatic considerations

and likely reflects more detailed molecular interactions between the bound formate ion and the closest solvent molecules. However, including explicit solvent molecules in the calculations incurs significant computational cost and is beyond the scope of the present work.

The CH stretching signatures of the bound formate ion exhibit solvatochromic blue shifts that increase with the dielectric constant of the solvent. This behavior can be traced to the change in the charge distribution of the formate ion upon solvation (Table 1), where the positive charge on the H atom increases in PCM calculations. The anomalously low value of the formate CH stretching vibration is due to an unusual, CH bond length-dependent mixing of different charge localization limits, and it has been shown to be strongly varying with the chemical environment of the ion.[39] Our observations of blue shifting CH stretching modes for both isomers, concomitant with a (calculated) increase in positive charge on the H atom, is consistent with an increased polarization of the charge distribution in the formate ion by interaction with the solvent, which can largely be captured by simple dielectric effects. We note that due to the poor solubility of formate salts in both acetone and acetonitrile (we did not observe any dissolution of salt crystals), we assume that neither of the CH stretching signatures originates from free formate in the solution.

Different from complexes of omC4P with nitrate or halide ions, there is a small (ca. 10 cm^{-1}) solvatochromic blue shift of the CH_3 stretching modes for $HCOO^-$·omC4P (Figure 4). Solvation seems to have little effect on the omC4P receptor itself in halide complexes. Therefore, we attribute this shift to the interaction between the bound ion and the methyl groups around the binding site, which is significantly stronger than for the other ions mentioned above. This shift is qualitatively recovered by PCM calculations (see Table 3), and it reflects the electrostatic interactions of the solvent and the bound ion, similar to the solvatochromic shifts of the formate CH stretching vibrations discussed above. We note that further investigation with a variety of solvents would be

interesting; however, as mentioned in earlier work,[15] effects of counter ions in solvents with low dielectric constants, H/D exchange in protic solvents, and strong solvent absorption peaks in the observed range in other cases precluded the use of other solvents.

Table 3. Selected Experimental Vibrational Frequencies of Formate-omC4P in cm^{-1} in Vacuo and the Relative Shifts of Equivalent Experimental and Scaled Harmonic Modes in CD_3CN and $(CD_3)_2CO$ solutions, in cm^{-1} from the Value in Vacuo.

In Vacuo	CD_3CN	PCM - CD_3CN			$(CD_3)_2CO$	PCM – $(CD_3)_2CO$		
		A	B	C		A	B	C
2665	28		83		21		80	
2754	26	-6		1	16	-9		-1
2868-2966[a]	10-12	30 - 26[b]	31 - 26[b]	27 - 23[b]	10-12	30 - 26[b]	31 - 26[b]	27 - 23[b]
3113	1	-18, 3 [d]	-18, 3 [d]	-14, 1 [d]	1	-18, 3 [d]	-18, 3 [d]	-14, 1 [d]
3250[a]	11[c]	-60, -28, 1[d]	1, 1[d]	-43, -23[d]	-6[c]	-59, -26, 3 [d]	-26, 3 [d]	-41, -19 [d]
3287	23[c]	-8	-8	-30	16[c]	4	-7	-27

[a] Peak centroid.

[b] Range of calculated features with this character.

[c] Values are the two features shown in Figure 4 fitted by two Gaussian profiles.

[d] Values separated by commas indicate different transitions contributing to one peak centroid.

Conclusions

The IR spectrum of formate complexed with omC4P shows that formate can bind in multiple different binding motifs with different H-bonding connectivity. One is characterized by a single oxygen interacting with three NH groups of omC4P and one oxygen interacting with the fourth NH group, another has one oxygen interacting with all four NH groups of the receptor, and the third exhibits two H-bonds for each of the two oxygen atoms. In each isomer, the symmetry of the molecule is broken from the C_{4v} symmetry observed in the halide-omC4P complexes to C_1, C_s, or C_{2v} symmetry due to the shape of the polyatomic guest ion. The existence of multiple isomers and the reduced symmetry is reflected in the broadening and pattern of the NH stretching features, which also encode the interaction between the formate ion and the omC4P binding site through their frequencies. These features are red-shifted from those in the spectrum of the analogous nitrate complex as expected from the higher proton affinity of formate compared to nitrate. The vibrational modes of the formate ion corroborate the identification of three separate host-guest binding motifs, as the formate CH stretching mode and the antisymmetric OCO stretching vibrational mode give rise to clearly separate features for the different isomers.

Solvent effects on the vibrational spectrum of $HCOO^-\cdot$omC4P are more complex than for other guest ions studied previously (halides, nitrate). The solvatochromic shifts of the formate CH stretching modes are consistent with a simple interpretation based on dielectric effects. However, the NH stretching modes of the omC4P host require a more nuanced picture, where effects of strong ion binding and the charge distribution that the bound formate ion presents to the chemical environment result in a more complex overall picture.

ASSOCIATED CONTENT

Supporting Information. The following files are available free of charge:

File 1: Experimental IR photodissociation spectrum of $HCOO^-$·omC4P compared to the scaled harmonic calculations of isomer A and isomer B; estimated energy barriers between isomer A and isomers B and C; ; mode patterns of NH stretching vibrational modes; atomic coordinates for neutral omC4P and for $HCOO^-$·omC4P.

File 2: Animation of the NH stretching mode with anharmonic behavior in isomer A and isomer B.

AUTHOR INFORMATION

Corresponding Author

*J. Mathias Weber – JILA and Department of Chemistry, University of Colorado, Boulder, Colorado 80309-0440, United States; orcid.org/0000-0002-5493-5886; Phone: +1-303-492-7841; Email: weberjm@jila.colorado.edu

Notes

The authors declare no competing financial interest.

ACKNOWLEDGMENT

J.M.W. gratefully acknowledges support by the National Science Foundation through the Division of Chemistry (award no. CHE-2154271) and through the JILA AMO Physics Frontiers Center (award no. PHY-2317149). This work utilized resources from the University of Colorado

Boulder Research Computing Group, which is supported by the National Science Foundation (awards ACI-1532235 and ACI-1532236), the University of Colorado Boulder, and Colorado State University.

REFERENCES

(1) Cremer, P. S.; Flood, A. H.; Gibb, B. C.; Mobley, D. L. Collaborative Routes to Clarifying the Murky Waters of Aqueous Supramolecular Chemistry. *Nat. Chem.* **2018**, *10*, 8.

(2) Dong, J.; Davis, A. P. Molecular Recognition Mediated by Hydrogen Bonding in Aqueous Media. *Angew. Chem., Int. Ed.* **2021**, *60*, 8035.

(3) Escobar, L.; Ballester, P. Molecular Recognition in Water Using Macrocyclic Synthetic Receptors. *Chem. Rev.* **2021**, *121*, 2445.

(4) Ariga, K.; Ito, H.; Hill, J. P.; Tsukube, H. Molecular recognition: from solution science to nano/materials technology. *Chem. Soc. Rev.* **2012**, *41*, 5800.

(5) Greer, M. A.; Goodman, G.; Pleus, R. C.; Greer, S. E. Health Effects Assessment for Environmental Perchlorate Contamination: The Dose Response for Inhibition of Thyroidal Radioiodine Uptake in Humans. *Environ. Health Perspect.* **2002**, *110*, 927.

(6) Kolesnichenko, I. V.; Anslyn, E. V. Practical Applications of Supramolecular Chemistry. *Chem. Soc. Rev.* **2017**, *46*, 2385.

(7) Kubik, S.; Reyheller, C.; Stüwe, S. Recognition of Anions by Synthetic Receptors in Aqueous Solution. *J. Incl. Phenom. Macrocycl. Chem.* **2005**, *52*, 137.

(8) Duax, W. L.; Griffin, J. F.; Langs, D. A.; Smith, G. D.; Grochulski, P.; Pletnev, V.; Ivanov, V. Molecular Structure and Mechanisms of Action of Cyclic and Linear Ion Transport Antibiotics. *Biopolymers* **1996**, *40*, 141.

(9) Martínez-Crespo, L.; Sun-Wang, J. L.; Sierra, A. F.; Aragay, G.; Errasti-Murugarren, E.; Bartoccioni, P.; Palacín, M.; Ballester, P. Facilitated Diffusion of Proline across Membranes of Liposomes and Living Cells by a Calix[4]pyrrole Cavitand. *Chem* **2020**, *6*, 3054-3070.

(10) Sato, E.; Hirata, K.; Lisy, J. M.; Ishiuchi, S.; Fujii, M. Rethinking Ion Transport by Ionophores: Experimental and Computational Investigation of Single Water Hydration in Valinomycin-K^+ Complexes. *J. Phys. Chem. Lett.* **2021**, *12*, 1754.

(11) Gale, P. A.; Sessler, J. L.; Král, V. Calixpyrroles. *Chem. Commun.* **1998**, 1.

(12) Gale, P. A.; Sessler, J. L.; Kral, V.; Lynch, V. Calix[4]pyrroles: Old Yet New Anion-Binding Agents. *J. Am. Chem. Soc.* **1996**, *118*, 5140.

(13) Dean, J. L. S.; Cramer, C. G.; Fournier, J. A. Interplay between Anion-Receptor and Anion-Solvent Interactions in Halide Receptor Complexes Characterized with Ultrafast Infrared Spectroscopies. *Phys. Chem. Chem. Phys.* **2024**, *26*, 21163.

(14) Cao, W.; Wang, X. Organic Molecules Mimic Alkali Metals Enabling Spontaneous Harpoon Reactions with Halogens. *Chem. Eur. J.* **2024**, *30*, e202400038.

(15) Terry, L. M.; Foreman, M. M.; Rasmussen, A. P.; McCoy, A. B.; Weber, J. M. Probing Ion-Receptor Interactions in Halide Complexes of Octamethyl Calix[4]Pyrrole. *J. Am. Chem. Soc.* **2024**, *146*, 12401.

(16) Baeyer, A. Ueber ein Condensationsproduct von Pyrrol mit Aceton. *Ber. Dtsch. Chem. Ges.* **1886**, *19*, 2184.

(17) Kim, D. S.; Sessler, J. L. Calix[4]pyrroles: Versatile Molecular Containers with Ion Transport, Recognition, and Molecular Switching Functions. *Chem. Soc. Rev.* **2015**, *44*, 532.

(18) Craig, S. M.; Menges, F. S.; Duong, C. H.; Denton, J. K.; Madison, L. R.; McCoy, A. B.; Johnson, M. A. Hidden Role of Intermolecular Proton Transfer in the Anomalously Diffuse Vibrational Spectrum of a Trapped Hydronium Ion. *Proc. Natl. Acad. Sci. U.S.A.* **2017**, *114*, E4706.

(19) Wada, K.; Kida, M.; Muramatsu, S.; Ebata, T.; Inokuchi, Y. Conformation of Alkali Metal Ion-Calix[4]Arene Complexes Investigated by IR Spectroscopy in the Gas Phase. *Phys. Chem. Chem. Phys.* **2019**, *21*, 17082.

(20) Foreman, M. M.; Hirsch, R. J.; Weber, J. M. Effects of Formate Binding to a Bipyridine-Based Cobalt-4N Complex. *J. Phys. Chem. A* **2021**, *125*, 7297.

(21) Inokuchi, Y.; Kusaka, R.; Ebata, T.; Boyarkin, O. V.; Rizzo, T. R. Laser Spectroscopic Study of Cold HostGuest Complexes of Crown Ethers in the Gas Phase. *ChemPhysChem* **2013**, *14*, 649.

(22) Terry, L. M.; Foreman, M. M.; Weber, J. M. Effects of Anion Size, Shape, and Solvation in Binding of Nitrate to Octamethyl Calix[4]pyrrole. *J. Phys. Chem. Lett.* **2024**, 9481.

(23) Xu, S.; Gozem, S.; Krylov, A. I.; Christopher, C. R.; Mathias Weber, J. Ligand influence on the electronic spectra of monocationic copper-bipyridine complexes. *Phys. Chem. Chem. Phys* **2015**, *17*, 31938.

(24) Chu, P. M., Guenther, F. R.; Rhoderick, G. C.; Lafferty, W. J. Quantitative Infrared Database. In *NIST Chemistry WebBook, NIST Standard Reference Database Number 69*, Mallard, P. J. L. a. W. G., Ed.: National Institute of Standards and Technology: Gaithersburg MD, 20899.

(25) Parr, R. G.; Yang, W. *Density-Functional Theory of Atoms and Molecules*; Oxford University Press, 1989.

(26) Becke, A. D. Density-Functional Exchange-Energy Approximation with Correct Asymptotic-Behavior. *Phys. Rev. A* **1988**, *38*, 3098-3100.

(27) Lee, C. T.; Yang, W. T.; Parr, R. G. Development of the Colle-Salvetti Correlation-Energy Formula into a Functional of the Electron-Density. *Phys. Rev. B* **1988**, *37*, 785-789.

(28) Dunning, T. H. Gaussian-Basis Sets for Use in Correlated Molecular Calculations .1. the Atoms Boron through Neon and Hydrogen. *J. Chem. Phys.* **1989**, *90*, 1007-1023.

(29) Barone, V. Anharmonic vibrational properties by a fully automated second-order perturbative approach. *J. Chem. Phys.* **2005**, *122*, 014108.

(30) Frisch, M. J.; Trucks, G. W.; Schlegel, H. B.; Scuseria, G. E.; Robb, M. A.; Cheeseman, J. R.; Scalmani, G.; Barone, V.; Petersson, G. A.; Nakatsuji, H.; et al. *Gaussian 16 Rev.* C.01, Wallingford, CT, 2016.

(31) Boys, S. F.; Bernardi, F. The calculation of small molecular interactions by the differences of separate total energies. Some procedures with reduced errors. *Mol. Phys.* **1970**, *19*, 553.

(32) Simon, S.; Duran, M.; Dannenberg, J. J. How does basis set superposition error change the potential surfaces for hydrogen-bonded dimers? *J. Chem. Phys.* **1996**, *105*, 11024.

(33) Glendening, E.; Reed, A.; Carpenter, J.; Weinhold, F. NBO, version 3.1, Gaussian. *Inc.: Pittsburgh, PA* **2003**.

(34) Miertuš, S.; Scrocco, E.; Tomasi, J. Electrostatic Interaction of a Solute with a Continuum. A Direct Utilization of Ab Initio Molecular Potentials for the Prevision of Solvent Effects. *Chem. Phys.* **1981**, *55*, 117.

(35) Davidson, J. A.; Fehsenfeld, F. C.; Howard, C. J. Heats of Formation of NO_3^- and NO_3^- Association Complexes with HNO_3 and HBr. *Int. J. Chem. Kinet.* **1977**, *9*, 17.

(36) Zagorec-Marks, W.; Foreman, M. M.; Verlet, J. R. R.; Weber, J. M. Probing the Microsolvation Environment of the Green Fluorescent Protein Chromophore. *J. Phys. Chem. Lett.* **2020**, *11*, 1940.

(37) Blodgett, K. N.; Fischer, J. L.; Zwier, T. S.; Sibert, E. L. The missing NH stretch fundamental in S(1)methyl anthranilate: IR-UV double resonance experiments and local mode theory. *Phys. Chem. Chem. Phys* **2020**, *22*, 14077.

(38) Schneider, H.; Vogelhuber, K. M.; Schinle, F.; Stanton, J. F.; Weber, J. M. Vibrational spectroscopy of nitroalkane chains using electron detachment and Ar predissociation. *J. Phys. Chem. A* **2008**, *112*, 7498.

(39) Gerardi, H. K.; DeBlase, A. F.; Su, X. G.; Jordan, K. D.; McCoy, A. B.; Johnson, M. A. Unraveling the Anomalous Solvatochromic Response of the Formate Ion Vibrational Spectrum: An Infrared, Ar-Tagging Study of the HCO_2^-, DCO_2^-, and $HCO_2^-\cdot H_2O$ Ions. *J. Phys. Chem. Lett.* **2011**, *2*, 2437.

TOC Graphic